Climate Dynamics
https://doi.org/10.1007/s00382-019-05091-7

Understanding the seasonal variations of Peninsular Florida

Vasubandhu Misra[1,2,3] · **Amit Bhardwaj**[1,3]

Received: 8 September 2019 / Accepted: 11 December 2019

Abstract
This study accounts for varying lengths of the seasons, which turns out to be an important consideration of climate variability over Peninsular Florida (PF). We introduce an objective definition for the onset and demise of the winter season over relatively homogenous regions within PF: North Florida (NF), Central Florida (CF), Southeast Florida (SeF), and Southwest Florida (SwF). We first define the summer season based on precipitation, and follow this by defining the winter season using surface temperature analysis. As a consequence, of these definitions of the summer and the winter seasons, the lengths of the transition seasons of spring and fall also vary from year to year. The onset date variations have a robust relationship with the corresponding seasonal length anomalies across PF for all seasons. Furthermore, with some exceptions, the onset date variations are associated with corresponding seasonal rainfall and surface temperature anomalies, which makes monitoring the onset date of the seasons a potentially useful predictor of the following evolution of the season. In many of these instances the demise date variations of the season also have a bearing on the preceding seasonal length and seasonal rainfall anomalies. However, we find that variations of the onset and the demise dates are independent of each other across PF and in all seasons. We also find that the iconic ENSO teleconnection over PF is exclusive to the seasonal rainfall anomalies and it does not affect the variations in the length of the winter season. Given these findings, we strongly suggest monitoring and predicting the variations in the lengths of the seasons over PF as it is not only an important metric of climate variability but also beneficial to reduce a variety of risks of impact of anomalous seasonal climate variations.

Keywords Climate · ENSO · Teleconnection · Interannual variability

1 Introduction

The boreal winter season of Florida is characteristically defined as a fixed length sequence of the calendar months of December–February (DJF; Winsberg 2003; Collins et al. 2019). In this study we introduce a new definition of the winter season over Peninsular Florida (PF) that accounts for varying length of the winter season from year to year. This study follows from our earlier work which defined the wet boreal summer season over PF (Misra et al. 2018). In that study we used area averaged rainfall over PF to define the onset date and the demise date of the summer season as the first and the last day when the cumulative anomaly curve of the daily rainfall reaches a minimum and a maximum in the year, respectively. The cumulative anomaly curve of the daily rainfall is defined by the running sum of the daily precipitation anomalies computed as the deviation from the corresponding climatological annual mean (Fig. 1 in Misra et al. 2018). Misra et al. (2018) clearly demonstrated that the onset and the demise of the PF wet season can be robustly defined by this method because of the strong seasonality in rainfall. Misra et al. (2018) showed that this seasonality of rainfall co-evolved with corresponding seasonal changes in the surrounding ocean surface temperatures and the loop current in the neighboring upper ocean. Furthermore, they also showed that the seasonality of the rainfall over PF is also associated with the corresponding seasonality of the upper-air wind circulation and atmospheric humidity gradients. However, the same methodology cannot be adopted to define the winter season of PF. This is because the winter season over PF is relatively drier and also exhibits a much

✉ Vasubandhu Misra
vmisra@fsu.edu

[1] Center for Ocean-Atmospheric Prediction Studies, Florida State University, Tallahassee, FL, USA

[2] Department of Earth, Ocean and Atmospheric Science, Florida State University, Tallahassee, FL, USA

[3] Florida Climate Institute, Florida State University, Tallahassee, FL, USA

Published online: 21 December 2019

stronger temporal variation, which causes ambiguous secondary minimum and maximum peaks in the cumulative anomaly curve of the daily rainfall.

The goals of this paper are to introduce the methodology of the diagnosis of the onset and the demise of the winter season, show the consistency of this definition of the winter season with other features in the atmospheric kinematic and thermodynamic fields, discuss the consequent shift in the seasonal cycle and its seasonal variations and prospects for predicting them. The winter season over PF is quite distinct in terms of the surface temperature (Winsberg 2003; Collins et al. 2019). It is marked by significant drop in surface temperature compared to the preceding fall and following spring seasons. The winter season over PF is comparatively drier and marked by frequent wildfires and episodic freeze events that cause widespread crop damage and vital economic loss to the state (Misra et al. 2017). The winter season over PF is also robustly teleconnected to El Niño and the Southern Oscillation (ENSO) in the equatorial Pacific (Ropelewski and Halpert 1986, 1987; Hansen et al. 1998; Stefanova et al. 2012; Nag et al. 2014). This teleconnection is widely known to suggest that warm and cold ENSO events usually produce cold/wet and warm/dry winters over PF, respectively. All of these teleconnection studies have invariably used fixed 3-month December–February (DJF) season to define the winter season over PF.

There is merit in investigating the variations in seasonal length. It is not obvious that climate variations have to necessarily follow the calendar months. Furthermore, conceiving a more objective definition of onset/demise of a season allows for potentially exploiting them as metrics for diagnosing model predictability. A practical advantage of defining a varying seasonal length is that it could also possibly lead to better energy and water management strategies as the source and consumption of these commodities are also seasonally dependent (Griffin and Chang 1991; Fazeli and Gillott 2013; Torriti 2017). As a consequence of defining the summer and the winter seasons over PF with varying lengths, the lengths of the transition fall and spring seasons will also vary. Therefore, any anticipated changes in the length of the forthcoming season over PF could be gainfully used for more optimal distribution and usage of the water and the energy resources. Scott et al. (2004) indicate that changes in seasonality due to climate change has a potential to affect tourism. They claim for example, that in a future warm climate, regions like south Florida and Arizona could face increasing holiday-maker competition for the winter sun, as more US cities become warmer and more desirable in the winter. By the same analogy, varying seasonal lengths can also regulate tourism in the current climate regime too if they are well anticipated. Additionally, the varying seasonal lengths can potentially help in understanding the changes in the phenology of the flora and fauna over PF. This is relevant to a region like Florida because of its unique geography that encompasses both temperate and sub-tropical climate regimes. As a consequence, Florida carries the largest number of plant families, highest number of fern species, has the highest diversity of orchid flora, and the densest concentration of carnivorous plant species in the United States and equally diverse wildlife (Knight et al. 2011; Stys et al. 2017).

In the following section we describe the data set and the methodology followed by the presentation of results in Sect. 3. The paper will conclude with some concluding remarks in Sect. 4.

2 Data and methodology

We make use of the daily surface temperature data available over global land surface regions made available by the Climate Prediction Center (CPC) of the National Centers for Environmental Prediction (NCEP), and obtained from https://www.esrl.noaa.gov/psd/data/gridded/data.cpc.globaltemp.html. This dataset is available globally over the land surface at $0.5^\circ \times 0.5^\circ$ spatial resolution from 1979 to 2018. This temperature data provides daily surface minimum (T_{min}) and maximum (T_{max}) temperatures. We made use of the T_{min} data. But using T_{max} did not change the diagnosis of the onset and demise date of the winter season (not shown). We also make use of the daily gridded precipitation data available over the continental US at $0.5^\circ \times 0.5^\circ$ spatial resolution from 1979 to 2018 following Xie et al. (2007) and Chen et al. (2008). In order to examine the upper air thermal and kinematic fields we made use of the climate forecast system reanalysis (CFSR; Saha et al. 2010). The CFSR data is available for the time period of 1979–2010 at $0.5^\circ \times 0.5^\circ$ grid resolution.

The diagnosis of the onset and the demise dates is restricted to PF and south of 30° N latitude. This is because north of 30° N the seasonality of precipitation is not strong (Misra and DiNapoli 2013; Misra et al. 2018). This consequently affects the determination of the onset and the demise of the winter season by the proposed methodology in this paper and hence the restriction to the domain outlined in Fig. 1. Figure 1 also show subdomains within PF: North Florida (NF), Central Florida (CF), Southwest Florida (SwF) and Southeast Florida (SeF). We will be diagnosing the onset/demise of the winter season uniquely for each of these subdomains. These subdomains were carefully considered so that each of these regions yielded distinct onset and demise dates of the summer and winter seasons for all years of the analysis. In going to finer spatial resolutions we encountered more uncertainty in the diagnosis of onset/demise dates of the summer season as a result of higher variance in the corresponding time series of daily rainfall. For example, the increased variance in the time series of rainfall aggregated to the county level yielded

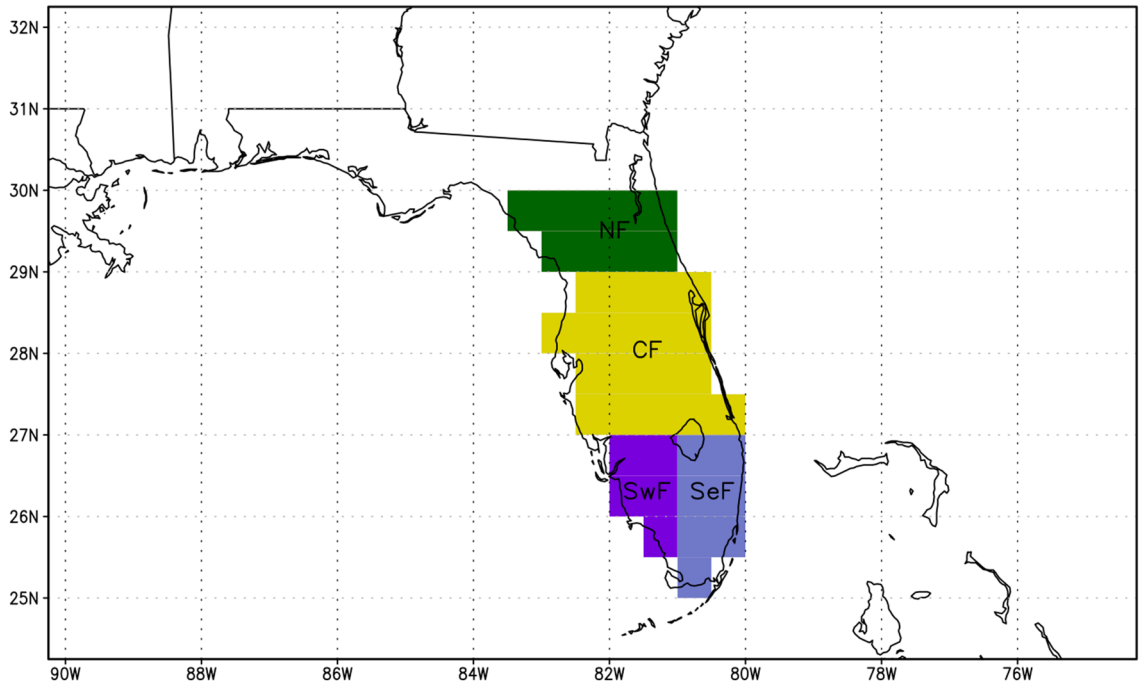

Fig. 1 The outline of the regional subdomains marking **a** North Florida (NF), **b** Central Florida (CF), **c** Southeast Florida (SeF), and **d** Southwest Florida (SwF)

uncertain estimates of the annual mean climatology, which in turn produced ambiguous diagnosis of the inflection points in the corresponding cumulative anomaly curve of rainfall. It is possible to overcome this shortcoming with possibly longer time series of the daily rainfall data to address the ambiguity of the diagnosis of the onset/demise dates of the summer season and consequently help with the definition of the winter season at higher spatial granularity when such data is made available. Furthermore, Misra and DiNapoli (2013) showed that the onset and demise of the summer season in SeF is distinct from SwF. We kept this in consideration to bifurcate south Florida into SwF and SeF as the onset/demise of the summer season consequently affects the length of the partial cumulative anomaly curve of surface minimum temperature for the diagnosis of the winter season.

In order to define the winter season, we initially have to obtain the onset and the demise date of the wet, summer season. This is easily done following Misra et al. (2018). The onset and the demise date of the summer season in each of the subdomains (see Fig. 1) is diagnosed as the minimum and the maximum in the daily cumulative anomaly curve of the corresponding area averaged rainfall, respectively. The cumulative daily anomaly of rainfall is given by:

$$R'_n(k) = \sum_{i=1}^{k} \left[R_n(i) - \overline{\overline{R}} \right] \tag{1}$$

where, $R_n(m)$ is the area averaged daily rainfall for day i of year n averaged separately over each of the subdomains of PF, $\overline{\overline{R}}$ is the corresponding annual mean climatology of the rainfall over the subdomain.

After the summer season is identified we take the area averaged daily time series of the $T_{\min}$ for each of the subdomains between the demise of the preceding summer season and the onset of the following summer season to compute the partial cumulative anomaly curve (PAC). This may be expressed mathematically for PAC of the *m*th Julian day for a given year as:

$$PAC\ (m) = \sum_{i=N}^{K} T'_{\min}(i) \tag{2}$$

where, i is the day of the year, N is the day of the demise of the preceding summer season and K is the day of the onset of the following summer season for the onset year of the winter season.

$$T'_{min}(i) = T_{\min}(i) - \bar{T}_{min} \tag{3}$$

And

$$\bar{T}_{min} = \frac{1}{L} \sum_{l=1}^{L} \frac{1}{J} \sum_{j=1}^{J} T_{min}(r,\ l) \tag{4}$$

$\bar{T}_{min}$ is the annual mean climatology of $T_{\min}$, L is the total number of years, and J is the number of days in the year.

It is important to compute the PAC (m) between N and K in Eq. (2) and not across the whole year because it results in unique inflection points in the PAC (Fig. 2). It may be noted that computing the cumulative anomaly curve with $T_{\min}$ for the whole year results in multiple inflection points that does not uniquely identify with a season. Figure 2 shows an example of the diagnosis of the onset and demise dates of the winter season of 1981–1982. The onset and the demise dates of the winter season is marked by the maximum and the minimum in the PAC curve (Fig. 2), respectively.

The significance of using different variables for defining the summer and the winter seasons over PF cannot be overemphasized. The summer season over PF is coincident with the rainy season and therefore justifies the use of precipitation to define the season following Misra et al. (2018). On the other hand, although the winter season is traditionally called the dry season (Winsberg 2003), it undergoes significant variations, particularly at interannual scales (Ropelewski and Halpert 1986, 1987; Nag et al. 2014). This variation renders some of the winter seasons over PF to have anomalous rainfall contrary to its "dry season" nomenclature. Therefore, our methodology fails to define unique (and objective) inflection points in the partial cumulative anomaly curve of precipitation for some of these relatively wet winter seasons. Alternatively, as proposed, PAC of the surface minimum temperature with its unique inflection points (Fig. 2) provides the desired objectivity to define the winter season. In the process of defining the winter season, which also requires the preceding summer season to be defined also in the process define the lengths of the transition spring and fall seasons. The onset of the spring and the fall seasons is the day after the demise of the winter and the summer seasons, respectively. Similarly, the demise of the spring and the fall seasons is marked by 1 day prior to the onset of the summer and the winter seasons, respectively.

In the following section we make use of the two tailed t test to assess the statistical significance as we present the results based on composite analysis and temporal correlations.

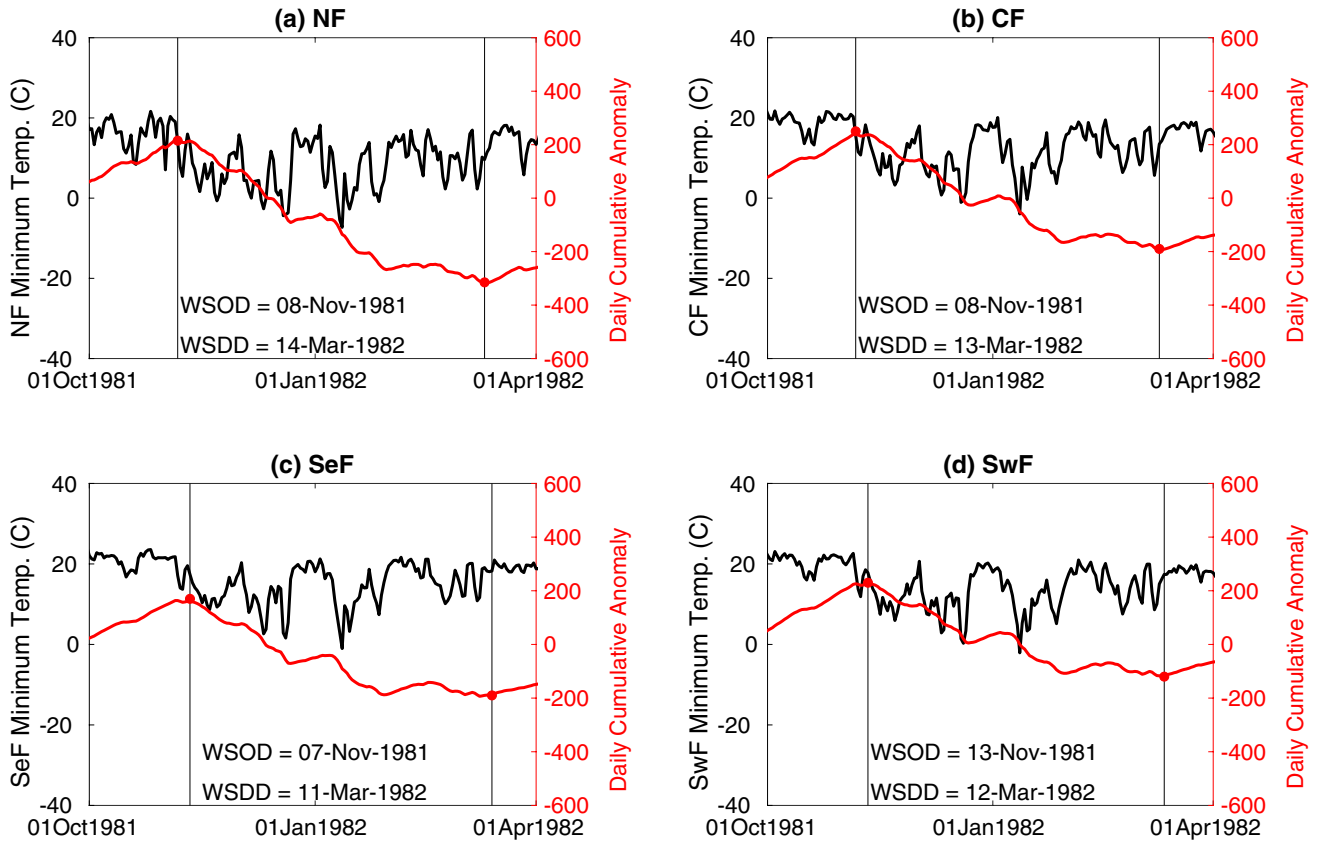

Fig. 2 Illustration of the diagnosis of onset and demise of the winter season over **a** NF, **b** CF, **c** SeF and **d** SwF for 1981–1982. The black curve in each of the panels is the daily surface temperature averaged over the regional subdomains between demise of the previous year (1981) and onset of the following year (1982) summer season in °C. The corresponding cumulative anomaly curve of the surface temperature is in red with onset date marked at nadir and demise date marked at zenith

3 Results

We will examine climatology of the seasons and the composite evolution of the winter season to examine the consistency of the methodology to diagnose the onset/demise of the season with respect to other variables. We will follow this presentation of results with the interannual variations in all four seasons.

3.1 Climatology of the seasons

The climatological onset dates, demise dates, and the length of the seasons for all four subdomains is shown in Table 1. This table shows that the onset/demise dates and the length of the winter season over SeF and SwF are comparable to each other. It may be noted that the standard deviation (σ) and the coefficient of variation of the length of the winter season ($=\frac{\sigma}{L}$; L is the climatological length of the season) in SeF is higher than that in SwF (Table 2). The coefficient of variation, which measures the dispersion around the mean thus suggests that the variations in the length of the winter season over SeF is more dominating than that over SwF (Table 2). However, as we proceed northward towards CF and NF, the length of the season progressively increases with earlier onset and later demise dates of the winter season relative to south Florida (SeF and SwF). Furthermore, the length of the winter season is longest over NF relative to the rest of the subdomains of PF (Table 2). From Table 1 it is also apparent that this new definition prolongs the winter season over all the subdomains of PF by nearly a month relative to the usual calendar months of DJF assigned to the winter season. Figure 3a–d and Table 2 indicate that the fall season is the shortest season over all subdomains of PF followed invariably by the spring season. There are however, a small minority of years when the summer season is shorter than the spring season in NF and SeF (Fig. 3a and c). The winter season is unambiguously the longest over NF and CF in all years (Fig. 3a and b). Table 2 clearly shows that the coefficient of variation of the length of the seasons over all of PF is significant, ranging anywhere from ~ 18 to 44%, which indicates that the variations of the seasonal length over PF is an important metric of climate variability in the region that cannot be ignored. Furthermore, generally, the fall season exhibits the largest coefficient of variation in its length followed by the spring season with the least coefficient of variation in the summer. Over NF, the coefficient of variation for the lengths of the summer and the winter seasons are comparable (Table 2).

3.2 The composite circulation around onset of the winter season

The diagnosis of the onset and the demise of the winter season is done through the surface temperature analysis and

Table 1 Climatological onset, demise, and length of the seasons over subdomains of Peninsular Florida

	Winter			Spring			Summer			Fall		
	Onset date	Demise date	Seasonal length (days)	Onset date	Demise date	Seasonal length (days)	Onset date	Demise date	Seasonal length (days)	Onset date	Demise date	Seasonal length (days)
NF	17 Nov	26 Mar	130	27 Mar	5 Jun	70	6 Jun	26 Sep	112	27 Sep	16 Nov	50
CF	22 Nov	26 Mar	125	27 Mar	1 Jun	66	2 Jun	3 Oct	123	4 Oct	21 Nov	48
SeF	28 Nov	21 Mar	114	22 Mar	28 May	67	29 May	6 Oct	130	7 Oct	27 Nov	51
SwF	26 Nov	21 Mar	116	22 Mar	27 May	66	28 May	6 Oct	131	7 Oct	25 Nov	49

Table 2 Climatology length (L; days), its standard deviation (σ; days), and coefficient of variation (C; %)

	Winter			Spring			Summer			Fall		
	L	σ	$C = \frac{\sigma}{L}$	L	σ	$C = \frac{\sigma}{L}$	L	σ	$C = \frac{\sigma}{L}$	L	σ	$C = \frac{\sigma}{L}$
NF	130	23	17.7	72	19	26.4	111	20	18	52	23	44.2
CF	125	25	20	67	21	31.3	123	19	15.4	48	18	37.5
SeF	114	32	28.1	69	25	36.2	130	24	18.5	53	22	41.5
SwF	116	25	21.6	67	19	28.4	130	16	12.3	50	22	44

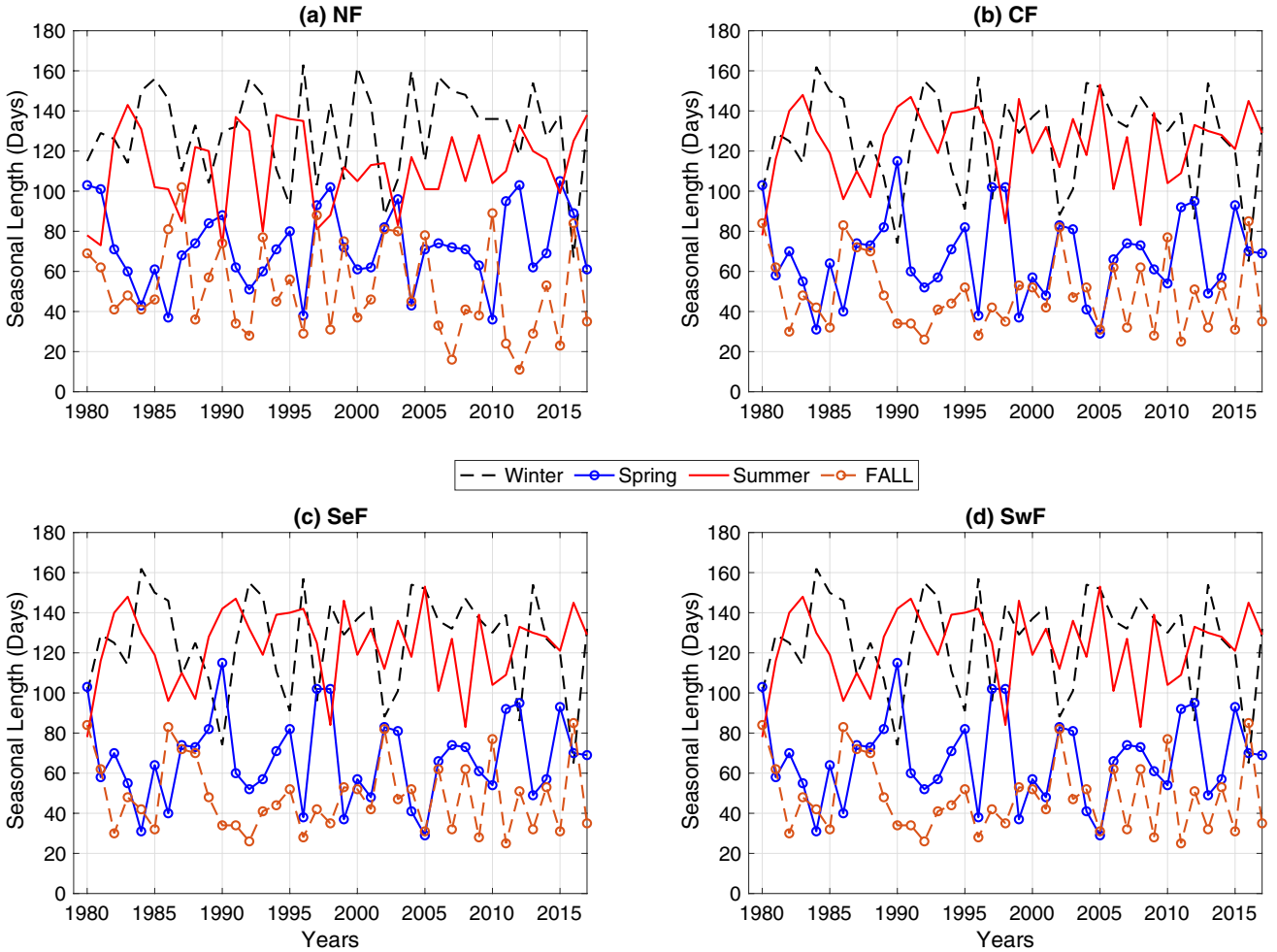

Fig. 3 The timeseries of the length of the seasons over **a** NF, **b** CF, **c** SeF, and **d** SwF. The units are in days

rainfall of the preceding summer season. In order to show the consistency of this diagnosis, we discuss in this subsection the composite circulation features associated with the diagnosed onset and the demise of the winter season over the region. The composite mean of the 850 hPa geopotential height, 200 hPa winds, and the mean sea level pressure (MSLP) at 5 day intervals on either side of the climatological onset of the winter season over CF is displayed in Fig. 4a–c. These composite means are qualitatively very similar when they are prepared relative to any of the other three subdomains (not shown). The composite is computed by taking the mean of these fields for each year on the corresponding day based on the onset of the year over CF. The MSLP in Fig. 4a shows that the surface anticyclone is centered over the tri-state region of Kentucky–Ohio–West Virginia, 5 days prior to the onset over CF. By the day of the onset (Fig. 4b), the surface anticyclone center strengthens and moves southwestward and is centered over Louisiana and the low pressure over the northeastern Atlantic region extends far down south. Five days after the onset (Fig. 4c), the anticyclone weakens relative to the day of the onset and the low MSLP over the eastern Atlantic nearly disappears.

This rapid southwestward displacement of the anticyclone is also noted in Davis et al. (1997). The upper air variables of 850 hPa geopotential height and 200 hPa winds show that on the day of the onset (Fig. 4b) the subtropical jet stream appears further south relative to its position 5 days before onset (Fig. 4a) and remains there at least 5 days post onset (Fig. 4c). However, the upper level winds and the geopotential height are more zonal at 5 days post onset (Fig. 4c). Furthermore, the meridional gradient of the geopotential field at 850 hPa is also the strongest at the time of the onset. Similarly, the large values of the upper-tropospheric (300–500 hPa layer) potential vorticity along the eastern seaboard including over PF, characterizes the trough as also evidenced in the 500 hPa (Fig. 4e) and the 850 hPa (Fig. 4b) geopotential heights on the day of the onset. The large values of the potential vorticity at onset would result in large values of cyclonic vorticity to compensate for the reduction in the stability of the air extruded from the stratosphere into the troposphere, which is prevalent in most mid-latitude weather systems during boreal winter season (Danielsen 1968; Hoskins et al. 1985). This is in contrast to the relatively quiescent composites 5 days prior (Fig. 4d) and post (Fig. 4f) onset of the winter season as evidenced by the smaller potential vorticity values over PF and the mid-Atlantic region. These composite figures (Fig. 4a–f) clearly suggest that the diagnosed onset of the winter season over CF is also characterized by the southward shift of the subtropical jet stream, stronger lower tropospheric thermal gradients and mid-level cyclonic flow that could amplify a frontal development.

3.3 The composite circulation around demise of the winter season

We plot in Fig. 5a–c the composite low level and upper level atmospheric variables at 5 day intervals centered around the demise date of the winter season over CF. The anticyclonic, surface high pressure centered over the southern Gulf coast 5 days prior to the demise date (Fig. 5a), transitions to the well-defined subtropical high pressure over the Atlantic Ocean by the day of the demise (Fig. 5b) and persists through at 5 days post demise (Fig. 5c). The 200 hPa winds and the 850 hPa geopotential heights indicate that the subtropical jet stream is receding further north gradually from 5 days prior to 5 days post demise of the winter season over CF (Fig. 5a–c). It is also apparent from these figures that the MSLP gradients which appeared to have stronger meridional gradients around the onset of the winter season (Fig. 4b, c) begins to transition, by having stronger zonal gradients, post demise of the winter season (Fig. 5b, c). This is also reflected in the 850 hPa geopotential height and 200 hPa winds when the implied thermal gradient and the winds relative to the onset period are weaker. The composite circulation in Fig. 5a–c indicate that the diagnosed demise of the winter season features a northward migration of the subtropical jet stream, weaker thermal gradients, and eastward migration of the north Atlantic subtropical high.

3.4 Interannual variability

The interannual variations of the seasonal length becomes an obvious metric to examine after the display of its relatively high coefficient of variation in Table 2. Figure 6 shows the correlation of the various parameters for all four seasons. We will examine each season separately in the following sub-sections.

3.4.1 Winter season

In all of the four sub-regions of PF the onset date strongly correlates with the corresponding length of the season (Fig. 6a–d). The relatively strong correlations imply that early or later onset of the winter season is associated with longer or shorter seasons, respectively. Likewise, early or later demise of the season is associated with shorter or longer seasonal length, respectively. But the onset and the demise date variations are insignificantly correlated to each other. Similarly, Fig. 6a–d suggests that early or later onset of the season is associated with corresponding drier or wetter seasonal rainfall anomalies, respectively. It may be however, noted that the correlations between the onset date variations and seasonal rainfall anomalies are weaker (but statistically significant) compared to that with the seasonal length. In contrast, the influence of the demise date variations on the seasonal rainfall anomalies is insignificant (Fig. 6a–d). The seasonal temperature anomalies are, however, shown not to display any significant relationship with variations in the length, onset date, demise date, and seasonal rainfall anomalies (Fig. 6a–d).

The winter ENSO teleconnections over PF are iconic for its robust relationship with rainfall anomalies (Ropelewski and Halpert 1986, 1987; Misra et al. 2017). We computed partial correlation ($\gamma_{ab/c}$; Eq. 5) to discern the impact of ENSO separately from the covariation of the onset date with other seasonal parameters of the winter season (Table 3). In Table 3, the Niño3.4 SST index is computed as an average over the 4 months of December through March to coincide with the diagnosed climatological length of the winter season (Table 1). The partial correlation is defined as:

$$\gamma_{ab/c} = \frac{\left[\gamma_{ab} - \gamma_{ac}\gamma_{bc}\right]}{\sqrt{1-\gamma_{ac}^2}\sqrt{1-\gamma_{bc}^2}} \tag{5}$$

where, $\gamma_{ab/c}$ is the correlation between two variables a and b after removing the influence of c on a and b. Similarly,

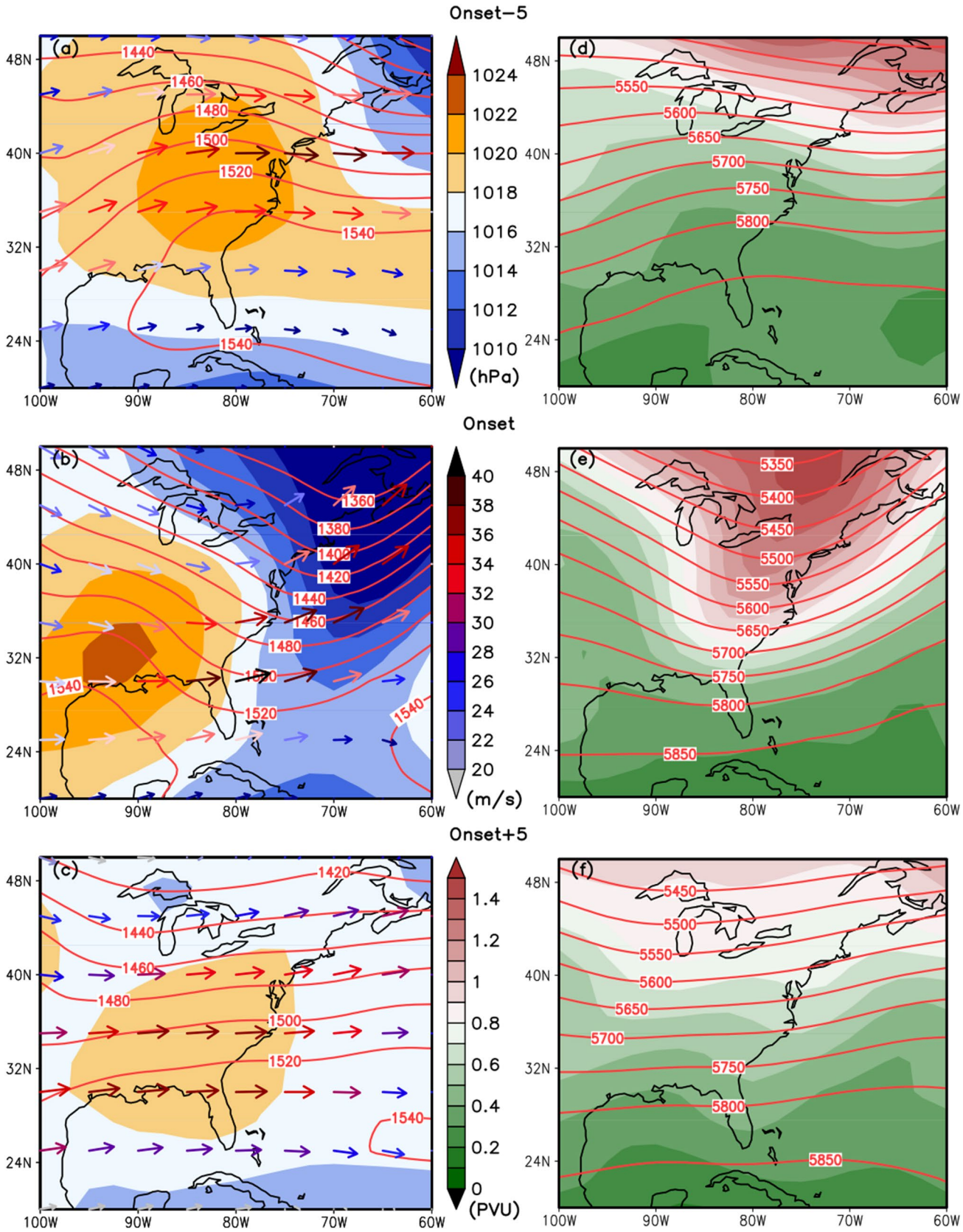
Onset−5
(a)
1440
1460
1480
1500
1520
1540
1540
(d)
5550
5600
5650
5700
5750
5800
1024
1022
1020
1018
1016
1014
1012
1010
(hPa)
Onset
(b)
1360
1380
1400
1420
1440
1460
1480
1500
1520
1540
1540
(e)
5350
5400
5450
5500
5550
5600
5650
5700
5750
5800
5850
40
38
36
34
32
30
28
26
24
22
20
(m/s)
Onset+5
(c)
1420
1440
1460
1480
1500
1520
1540
(f)
5450
5500
5550
5600
5650
5700
5750
5800
5850
1.4
1.2
1
0.8
0.6
0.4
0.2
0
(PVU)
48N
40N
32N
24N
100W
90W
80W
70W
60W

◂**Fig. 4** Composite of the 850 hPa geopotential height field (m; Red contours), winds at 200 hPa (vectors; m/s), and mean sea level pressure (shaded; hPa) at **a** 5 days before climatological onset, **b** climatological onset, and **c** 5 days after climatological onset of the winter season. Similarly, composites of the 500 hPa geopotential height field (Red contours) and potential vorticity in the 300–500 hPa layer (PVU [$=10^{-6}$ K kg^{-1} m^2 s^{-1}]; shaded) at **d** 5 days before climatological onset, **e** climatological onset, and **f** 5 days after climatological onset of the winter season. The composites shown pass the significance test at 10% significance level according to *t* test

$\gamma_{ab}, \gamma_{ac}, \gamma_{bc}$ are correlations between variables a and b, a and c, and b and c respectively. In Table 3, using Eq. (5), we uniquely determine the influence of ENSO and onset date variations (after removing the influences between them) on the seasonal rainfall, seasonal temperature, seasonal length, and the demise date of the winter season over all four subdomains of PF. Table 3 suggests that onset date variations uniquely influence (outside of ENSO variability) the seasonal length variations. For example, Table 3 indicate that early onset leads to corresponding longer winter seasons in all the four subdomains. Likewise, warm or cold ENSO anomalies lead to wetter or drier winter anomalies over all subdomains of PF (Table 3). But onset date variations in the absence of the ENSO influence also affect the seasonal winter rainfall variations over SwF only (Table 3). At this time we are unable to explain this unique feature of winter rainfall variations of SwF. However, this result further justifies in identifying SwF as a subdomain, distinct from other regions of PF. The partial correlation analysis in Table 3 suggests that ENSO teleconnections does not impact variations in the onset, demise, or the length of the winter season over PF. Furthermore, the correlations of the onset date with the seasonal rainfall anomalies observed earlier in Fig. 6a–d disappears in all the subdomains after the ENSO influence is removed except over the SwF. This suggests that onset date variations provide an independent and additional predictor for winter seasonal rainfall anomalies over SwF besides ENSO variations. In the other subdomains it is the influence of ENSO that allows for the co-variability between the onset date variations and the corresponding seasonal winter rainfall anomalies.

3.4.2 Spring season

The spring season displays a relatively strong correlation between the variations of the onset date with variations of the corresponding seasonal length and seasonal temperature anomalies (Fig. 6e–h). These correlations, for example, suggest that early onset of the season lead to longer and cooler spring seasons. The onset date variations of the spring season, however, does not have a significant relationship with the corresponding seasonal rainfall anomalies. The demise date variations, however, show strong relationship with the seasonal rainfall anomalies and slightly weaker but statistically significant relationship with surface temperature and seasonal length anomalies. For example, later demise of the spring season is likely to be associated with longer, wetter, and warmer seasonal anomalies. But the onset date and demise date variations seem to be independent of each other with their lack of significant correlation. The spring season, unlike the winter season shows a statistically significant positive correlation between surface temperature and rainfall anomalies over all subdomains except over CF.

3.4.3 Summer season

In contrast to the winter season, the onset date variations of the summer season have a bearing on the corresponding seasonal length, rainfall, and surface temperature anomalies over all the subdomains in PF (Fig. 6i–l). These correlations suggest for example, that early onset of the season leads to the greater likelihood of longer, wetter, and cooler summer season. Similarly, the demise date of the season also displays a strong influence on the evolution of the seasonal anomalies (Fig. 6i–l). For example, early demise of the season is associated with shorter, drier, and warmer summer seasonal anomalies. It may, however, be noted that the relationship of the demise date variations with the summer seasonal surface temperature anomalies over south Florida is weak and insignificant. In addition, the demise date and onset date variations are also poorly correlated. The seasonal length anomalies are also strongly related to the corresponding seasonal rainfall anomalies but not with seasonal temperature anomalies (Fig. 6i–l). These correlations imply that longer or shorter seasons are associated with wetter or drier summers, respectively.

3.4.4 Fall season

The fall season also exhibits a strong association of the onset date variations with the corresponding seasonal length, rainfall, and surface temperature anomalies over all of PF (Fig. 6m–p). For example, early onset of the season leads to greater likelihood of longer, drier, and warmer fall season across PF. Although the demise date variations show a strong relationship with seasonal length anomalies, its relationship with seasonal rainfall and temperature anomalies are much weaker (but statistically significant) than that of the onset date variations. The seasonal length anomalies show a robust relationship with seasonal rainfall anomalies, showing longer or shorter seasons to be likely associated with wetter or drier fall seasons, respectively. However, such relationship is absent with surface temperature anomalies (Fig. 6m–p). Once again, we observe that the onset and the demise date variations are insignificantly related to each other.

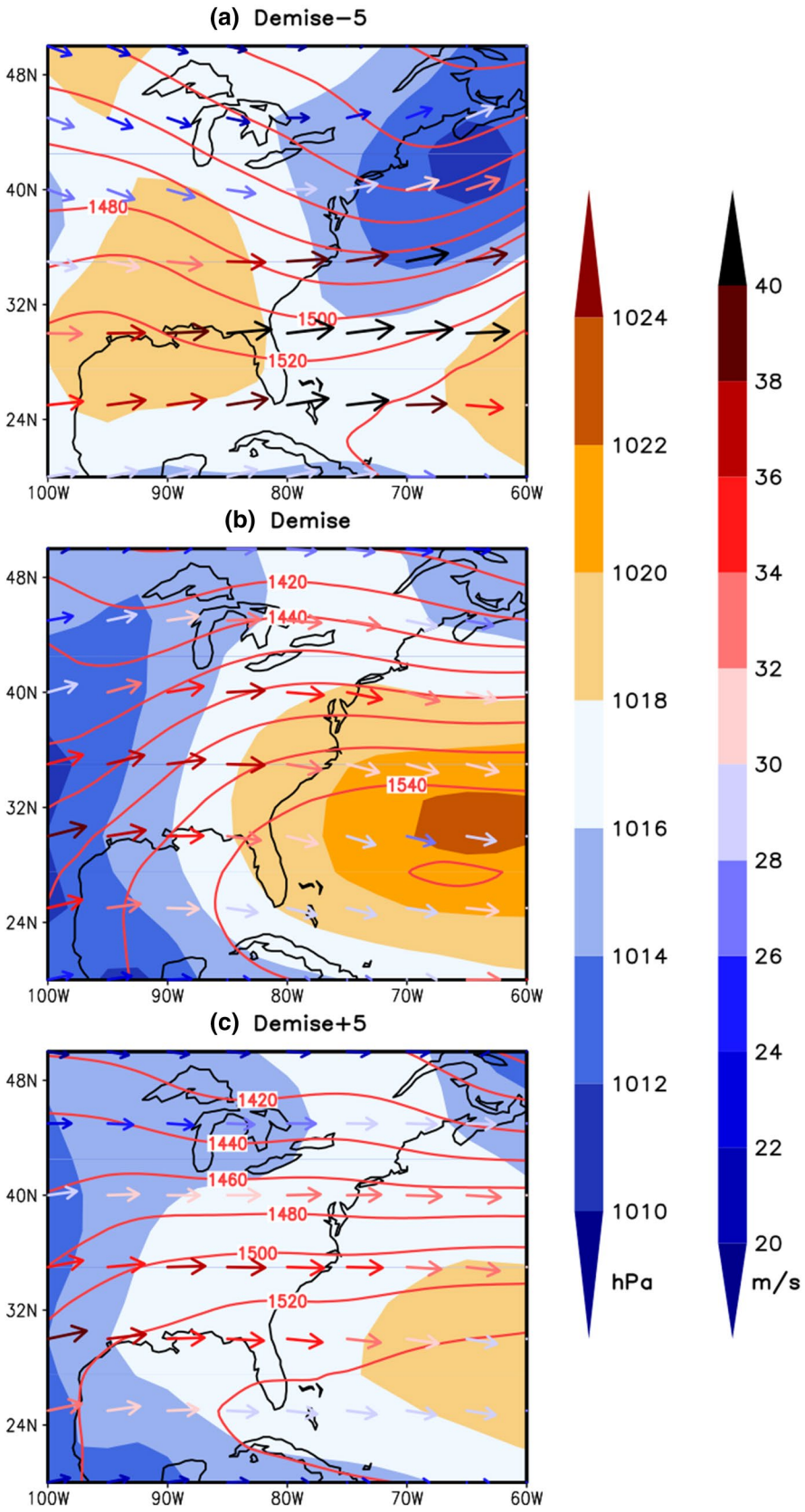

Fig. 5 Composite of the 500 hPa geopotential height field (contoured), winds at 200 hPa (vectors; m/s), and mean sea level pressure (shaded; hPa) at **a** 5 days before climatological demise, **b** climatological demise, and **c** 5 days after climatological demise of the winter season. The thick black line shows the climatological freezing line at surface. The composites shown pass the significance test at 10% significance level according to *t* test

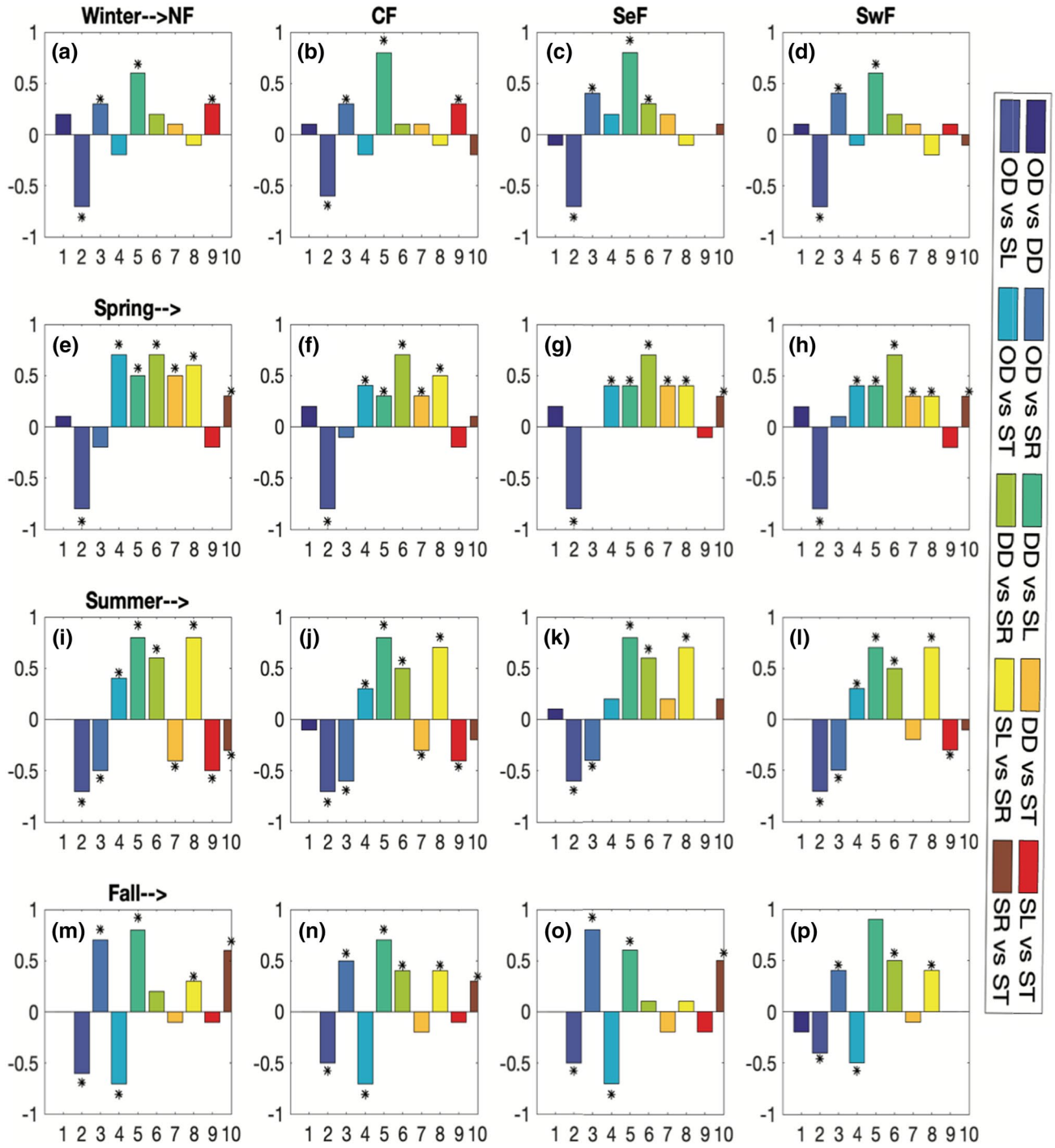

Fig. 6 The correlations between the various variables of the season for **a**–**d** Winter, **e**–**h** Spring, **i**–**l** Summer, and **m**–**p** Fall seasons over (**a**, **e**, **i**, **m**) NF, (**b**, **f**, **j**, **n**) CF, (**c**, **g**, **k**, **o**) SeF, and (**d**, **h**, **l**, **p**) SwF. The variables are *OD* onset date, *DD* demise date, *SL* seasonal length, *SR* seasonal rainfall, *ST* seasonal surface temperature. The correlations, which are statistically significant at 10% significance level according to *t* test are indicated by a black asterisk on top of each bar

4 Conclusions

This work clearly indicates that variations in the length of the seasons is an important consideration of climate variability over PF. In this study, we have introduced an objective definition for defining the onset, demise, and therefore the length of the winter season for the four subdomains of PF (NF, CF, SeF, SwF). This definition of the winter season although is

Table 3 Partial correlation analysis of the winter season over Peninsular Florida

	Seasonal rainfall		Seasonal temperature		Seasonal length		Demise date	
	With only Niño3.4	With only onset date	With only Niño3.4	With only onset date	With only Niño3.4	With only onset date	With only Niño3.4	With only onset date
NF	**0.5**	0.2	−0.03	−0.2	−0.02	**−0.7**	-0.02	0.2
CF	**0.7**	0.2	−0.03	−0.2	0.02	**−0.5**	0.02	0.1
SeF	**0.7**	0.2	−0.01	0.2	0.2	**−0.7**	0.2	−0.1
SwF	**0.8**	**0.3**	0.02	−0.1	0.1	**−0.7**	0.1	0.1

Bold values are significant at 90% confidence interval according to *t* test

derived from surface temperature and precipitation of the preceding summer season, it is shown to have consistency with the evolving thermodynamic and kinematic fields of the upper air.

The traditional definition of pegging the boreal winter season over PF to calendar dates of December 1 to February 28/29, limits the variability of the season. We are able to leverage the strong seasonality of the hydroclimate in PF to first define the summer season and thereafter use the variations in the surface temperature to define the winter season. As a result of defining the summer and winter seasons of varying length, the remaining two seasons are also altered, with the fall season being consistently the shortest of the four seasons over PF.

The highlight of the introduced methodology to diagnose the onset/demise of the winter season over PF is its simplicity. It uses daily surface temperature and rainfall analysis, which is easily available for PF. Furthermore, the methodology involves simple linear operations that can easily be accomplished without significant effort. In addition, the diagnosed dates of onset and demise of the winter season is shown to be consistent with the evolution of the atmospheric kinematic and thermodynamic fields. We have likewise shown similar consistency in the diagnosis of the onset/demise of the summer season in Misra et al. (2018). The results of this study are also significant in that the coefficient of variation of the seasonal length is relatively large ranging from ~ 18 to 44% across all four seasons over PF. The fall season shows the highest coefficient of variation followed by the spring season, with the summer showing the least across all four subdomains of PF. Therefore, it is important to acknowledge the variations in the length of the seasons over PF while assessing the climate variability of the region.

The analysis of the interannual variations indicate that onset date variations have a robust relationship with the corresponding seasonal length anomalies across PF for all seasons. Furthermore, with some exceptions (as discussed in Sect. 3.1), the onset date variations are associated with corresponding seasonal rainfall and surface temperature anomalies. These results suggest that monitoring the onset date of the seasons can be a useful predictor of the following evolution of the season. In many of these instances the demise date variations of the season also have a bearing on the preceding seasonal length and rainfall anomalies. However, we find that variations of the onset and demise date are independent of each other across PF and in all seasons. We also find that the iconic ENSO teleconnection over PF is exclusive to the seasonal rainfall anomalies and it does not affect the variations in the length of the winter season nor its onset/demise dates.

A summary of the important results from this study are:

- Climatologically, the fall season is the shortest across PF. The winter season over NF and CF and the summer season over SwF and SeF is the longest season.
- The coefficient of variation in the length of the season over PF ranges from 18 to 44% with fall season having the largest followed by that in the spring with the summer displaying the least.
- The interannual variations of the winter seasonal rainfall anomaly across PF is largely dictated by ENSO variations.
- The interannual variations of the seasonal length of the winter, spring, summer and fall seasons are significantly associated with the variations of their corresponding date of onset of the season over all subdomains of PF. Additionally, in the case of all seasons except for the winter, the onset date variations is also found to be significantly associated with the corresponding seasonal rainfall and temperature anomalies across PF.

Although our study clearly demonstrates the importance of accounting for the variations in the length of the seasons over PF to account for the climate variability, it becomes a challenge to diagnose these variations when daily data of surface temperature and rainfall is not available. We cannot offer a recourse for instances where only monthly data is available except to acknowledge that climatologically, it is seen from our definition that over PF the winter, spring, summer, and fall seasons is approximately December through March, April through May, June through September, and October through November, respectively. But with cheaper storage space, improved analysis of observations, and data available from a newer generation of models it is

now more likely than ever that daily data of some of these surface variables are more readily available. Our future work involves examining the seasonal predictability of the onset and demise of the seasons and also examining the impact of climate change on the variations of the length of the seasons over PF.

Acknowledgements The authors gratefully acknowledge the financial support given by NASA Grants NNX17AG72G, NNX16AD83G, NSF Award No. 1606296. We also acknowledge the help of two anonymous reviewers who provided with very useful comments on an earlier version of this manuscript.

References

Chen M, Shi W, Xie P, Silva VB, Kousky VE, Wayne-Higgins R, Janowiak JE (2008) Assessing objective techniques for gauge-based analyses of global daily precipitation. J Geophys Research Atmos. https://doi.org/10.1029/2007JD009132

Collins J, Rohli RV, Paxton CH (2019) Florida weather and climate: more than just sunshine. University Press of Florida, Gainesville, p 247

Danielsen EF (1968) Stratosphere-troposphere exchange based on radioactivity, ozone, and potential vorticity. J Atmos Sci 25:502–518. https://doi.org/10.1175/1520-0469(1968)025%3c0502:STEBOR%3e2.0.CO;2

Davis RE, Hayden BP, Gay DA, Phillips WL, Jones GV (1997) The North Atlantic subtropical anticyclone. J Clim 10:728–744. https://experts.illinois.edu/en/publications/the-north-atlantic-subtropical-anticyclone. Accessed 1 Feb 2019

Fazeli A, Gillott M (2013) Analysing the effects of seasonal variation on occupancy in an electricity demand model. Int J Low Carbon Technol 8:282–288. https://doi.org/10.1093/ijlct/cts032

Griffin RC, Chang C (1991) Seasonality in community water demand. Western J Agric Econ 16:207–217. https://ideas.repec.org/a/ags/wjagec/32611.html. Accessed 20 Jan 2019

Hansen JW, Hodges AW, Jones JW (1998) ENSO Influences on agriculture in the Southeastern United States. J Clim 11(3):404–411

Hoskins BJ, McIntyre ME, Robertson AW (1985) On the use and significance of isentropic potential vorticity maps. Q J R Meteorol Soc. 111:877–946. https://doi.org/10.1002/qj.49711147002

Knight GR, Oetting JB, Cross L (2011) Atlas of Florida's natural heritage -biodiversity, landscapes, stewardship, and opportunities. Institute of Science and Public Affairs, Florida State University, Tallahassee, FL. http://www.floridasnaturalheritage.org/. Accessed 19 May 2019

Misra V, DiNapoli SM (2013) Understanding the wet season variations over Florida. Clim Dyn 40:1361–1372. https://doi.org/10.1007/s00382-012-1382-4

Misra V, Selman C, Waite AJ, Bastola S, Mishra A (2017) Terrestrial and ocean climate of the 20th century. In: Chassignet EP, Jones JW, Misra V, Obeysekera J (eds) Florida's climate: changes, variations and impacts. Florida Climate Institute, Florida, pp 330–389. https://doi.org/10.17125/fci2017.ch16

Misra V, Bhardwaj A, Mishra A (2018) Characterizing the rainy season of Peninsular Florida. Clim Dyn 51:2151–2157. https://doi.org/10.1007/s00382-017-4005-2

Nag B, Misra V, Bastola S (2014) Validating ENSO teleconnections on Southeastern United States winter hydrology. Earth Interact. https://doi.org/10.1175/EI-D-14-0007.1

Ropelewski CF, Halpert MS (1986) North American precipitation and temperature patterns associated with the El Nino/Southern Oscillation (ENSO). Mon Weather Rev. 114:2352–2362. https://doi.org/10.1175/1520-0493(1986)114%3c2352:NAPATP%3e2.0.CO;2

Ropelewski CF, Halpert MS (1987) Global and regional scale precipitation patterns associated with the El Nino/Southern Oscillation. Mon Weather Rev. 115:1606–1626. https://doi.org/10.1175/1520-0493(1987)115%3c1606:GARSPP%3e2.0.CO;2

Saha S, Moorthi S, Pan HL, Wu X, Wang J, Nadiga S, Tripp P, Kistler R, Woollen J, Behringer D, Liu H (2010) The NCEP climate forecast system reanalysis. Bull Am Meteorol Soc 91(8):1015–1057

Scott D, McBoyle G, Schwartzentruber M (2004) Climate change and the distribution of climatic resources for tourism in North America. Clim Res 27:105–117. https://doi.org/10.3354/cr027105

Stefanova L, Misra V, Chan S, O'Brien JJ, Smith TJ III (2012) A proxy for high resolution regional reanalysis for the Southeast United States: assessment of precipitation variability. Clim Dyn. https://doi.org/10.1007/s00382-011-1230-7

Stys B, Foster T, Fuentes MMPB, Glazer B, Karish K, Montero N, Reece JS (2017) Climate change impacts on Florida's biodiversity and ecology. In: Chassignet EP, Jones JW, Misra V, Obeysekera J (eds) Florida's climate: changes, variations and impacts. Florida Climate Institute, Florida, pp 339–389. https://doi.org/10.17125/fci2017.ch12

Torriti J (2017) Understanding the timing of energy demand through time use data: time of the day dependence of social practices. Energy Res Soc Sci 25:37–47. https://doi.org/10.1016/j.erss.2016.12.004

Winsberg MD (2003) Florida weather. The University Press of Florida, Florida, p 218

Xie P, Yatagai A, Chen M, Hayasaka T, Fukushima Y, Liu C, Yang S (2007) A gauge-based analysis of daily precipitation over East Asia. J Hydrometeorol 8:607–626. https://doi.org/10.1175/JHM583.1